

Simulating one hundred entangled atoms using projected-interacting full configuration interaction wavefunctions corrected by projected density functionals

Benjamin G. Janesko

Department of Chemistry & Biochemistry, Texas Christian University, Fort Worth, TX 76129, USA.

b.janesko@tcu.edu

Abstract

Simulating entangled atoms is a prerequisite to modeling quantum materials and remains an outstanding challenge for theory. I introduce a correlated wavefunction approach capable of simulating large entangled systems, and demonstrate its application to a 300-electron active space. Projected-interacting full configuration interaction plus density functional theory PiFCI+DFT combines near-exact correlated wavefunctions of multiple partially-interacting model systems, each corrected by a formally exact density functional. This approach can access large active spaces and visualize entanglement and strong correlation while maintaining competitive accuracy for molecular properties.

Introduction

Quantum materials exploit quantum entanglement to provide unique properties, including high-temperature superconductivity, beyond-classical measurement sensitivity, and switchable qubits for quantum computing.¹ The textbook example of quantum entanglement is the double-slit experiment (Figure 1a). A single incident electron is “shared” between two slits in a mask, yielding quantum interference in the transmitted electron’s probability distribution. (“Sharing” means that the expectation value of each slit’s population is not one of the eigenfunctions (0,1,2...) of the population operator.) Measuring one slit’s population collapses the wavefunction and eliminates the quantum interference. Many quantum materials share *multiple* electrons among entangled atoms. The diamond nitrogen-vacancy defect (NV⁻), an optically addressable qubit and quantum sensor, shares six electrons among four entangled atoms surrounding the vacancy.² High-temperature superconductivity is hypothesized to arise from strongly correlated electron processes involving large numbers of entangled atoms.³ Entangled atoms can also occur in chemical reactions. The dissociating hydrogen dimer cation H_2^+ shares a single electron among two entangled hydrogen nuclei, a molecular analogue of the double-slit experiment. The dissociating ground-state singlet nitrogen molecule N_2 (Figure 1b) shares six electrons among two entangled atoms.

While the double-slit experiment is a staple of undergraduate physics, simulating *multiple-electron* entanglement in quantum materials is a major challenge. The wavefunctions of “normal” molecules and solids are well-approximated by a single molecular orbital configuration (single Slater determinant).⁴ The wavefunctions of entangled many-electron systems may instead require a very large number of configurations. For example, a minimal complete active space (CAS) wavefunction of M entangled nitrogen atoms includes on the order of $(3M)!$ configurations: all the ways to distribute $3M$ bonding electrons among $6M$ spin-orbitals. Six atoms require more than a mole of configurations! Figure 2a illustrates this imbalance for N_2 dissociation. The figure shows dissociation curves computed with four approximate wavefunctions: single-configuration

entangled (RHF singlet), ten-configuration entangled (CAS(6,6)SCF singlet), single-configuration unentangled (UHF hexet), and accurate multireference NEVPT2⁵. RHF is qualitatively reasonable for “normal” N₂ near equilibrium, but awful at dissociation. Even *computing* the RHF wavefunction is difficult due to variational collapse into artificially stabilized unentangled symmetry broken states.⁶ While significant progress has been made, simulating strong correlation remains a significant challenge. State-of-the-art GPU-accelerated multireference methods running on classical computers⁷ top out at about 100 strongly correlated electrons.⁸⁻⁹

Kohn-Sham density functional theory (KS-DFT) provides an alternative. For a system of *noninteracting* electrons, entangled or not, the exact wavefunction is a single molecular orbital configuration (apart from some edge cases¹⁰⁻¹¹). DFT predicts a real system’s ground-state energy and density from a model system of noninteracting electrons, corrected by a formally exact density functional. State-of-the-art DFT codes can treat millions of atoms,¹² raising the prospect of modeling millions of *entangled* atoms. Unfortunately, the exact functional is unknown, and existing approximate functionals struggle to treat strong correlation¹³ (e.g., the flat-plane condition¹⁴⁻¹⁶). The PBE0¹⁷⁻¹⁹ results in Figure 2a exemplify standard DFT. The bond energy near equilibrium is very accurate, but the energy at dissociation is not. Standard approximate functionals also give a “zero-sum” tradeoff between underestimated strong correlation and over-delocalization of charge and spin (Figure SI1).²⁰ Symmetry breaking can recover accurate energies at dissociation, but lose the entanglement of the reference system wavefunction.⁶ Modern flat-plane functionals can be near-exact for model systems at dissociation,²¹ but may be unreliable for interacting entangled quantum materials. All of this motivates the present work.

PiFCI+DFT

I introduce projected-interacting full configuration interaction plus density functional theory PiFCI+DFT. The thick black curves in Figure 2 show the results. Figure 3 shows the idea. Rather than computing an extremely expensive wavefunction for the interacting-electron system (Figure 3 top), or relying completely on an approximate density functional to correct a noninteracting-electron reference system (Figure 3 middle), I compute and combine *modestly expensive and nearly exact* wavefunctions of multiple projected-interacting reference systems. The approach builds on Hubbard DFT+U²² and the extension of KS-DFT to partially interacting reference systems.²³⁻²⁵ I define multiple reference systems, each including an electron-electron interaction projected onto a single state $|\phi_n\rangle$ (eq 1). The bottom panel of Figure 3 illustrates one of these states for N₁₀. The real system’s exact ground-state energy and density may be obtained from the noninteracting KS-DFT reference system (eq 2), or from any one of the partially interacting reference systems (eq 3), each corrected by a Hartree-exchange-correlation (HXC) density functional. The Hohenberg-Kohn theorems guarantee these functionals’ existence.²³ Functional $E^{\text{KS}_{\text{HXC}}}[\rho]$ corrects the noninteracting KS reference system, projected functional $E^{\text{P},n}_{\text{HXC}}[\rho]$ corrects the n th partially interacting reference system.²⁵ Given the exact functionals, any weighted sum of the reference systems (eq 4) *also* gives the exact result. (I assume the exact ground-state density is noninteracting v -representable and projected-interacting v -representable, i.e., that it is a possible ground-state density of every reference system.) One can choose the states and weights

$|\phi_n\rangle, w_n$ so that accurate calculations on the projected-interacting reference systems compensate for the limitations of approximate density functionals.

$$\begin{aligned}
 (1) \quad \widehat{V}_{ee}^{P,n} &= |\phi_n \phi_n\rangle U_n \langle \phi_n \phi_n|; \quad U_n = \langle \phi_n \phi_n | \widehat{V}_{ee} | \phi_n \phi_n \rangle \\
 (2) \quad E_{KS}[\rho] &= \min_{\Phi \rightarrow \rho} \langle \Phi | \hat{T} | \Phi \rangle + \int d^3\vec{r} \, v(\vec{r})\rho(\vec{r}) + E_{HXC}^{KS}[\rho] \\
 (3) \quad E_{P,n}[\rho] &= \min_{\Psi \rightarrow \rho} \langle \Psi | \hat{T} + \widehat{V}_{ee}^{P,n} | \Psi \rangle + \int d^3\vec{r} \, v(\vec{r})\rho(\vec{r}) + E_{HXC}^{P,n}[\rho] \\
 (4) \quad E &= \min_{\rho} \left\{ E_{KS}[\rho] + \sum_n w_n (E_{P,n}[\rho] - E_{KS}[\rho]) \right\}
 \end{aligned}$$

PiFCI+DFT requires choices. The choices I make here are “black-box”, and do not require the user to preselect active spaces, weights, or other system-dependent parameters. I’ll discuss each choice in turn.

Reference System Full CI. If a system’s electron-electron interaction is projected onto a single normalized state (eq 1), the system’s full configuration interaction ground-state wavefunction requires at most two Slater determinants.²⁶ Briefly, starting from the single-determinant reference wavefunction $|\Phi_0\rangle$, separate unitary transforms of the occupied and virtual spaces ensure that only one transformed occupied spinorbital $|\psi_{o\sigma}\rangle$ and one transformed unoccupied spinorbital $|\psi_{v\sigma}\rangle$ have nonzero projections onto $|\phi_n\rangle$. These projections define *occupation numbers* similar to those used in DFT+U: $|\langle \psi_{o\sigma} | \phi_n \rangle|^2 = n_{p\sigma}$, $|\langle \psi_{v\sigma} | \phi_n \rangle|^2 = n_{p\sigma}^v$. (If the spinorbitals are expanded in a complete one-electron basis set, then $n_{p\sigma} + n_{p\sigma}^v = 1$.) The bottom panel of Figure 3 illustrates the projection state (black) and transformed orbitals for one of the 40 reference systems used to model N₁₀. The reference system full CI wavefunction includes only two Slater determinants $|\Phi_0\rangle$ and $|\Phi_{oo}^{vv}\rangle$. The latter replaces each $|\psi_{o\sigma}\rangle$ in $|\Phi_0\rangle$ with $|\psi_{v\sigma}\rangle$. The off-diagonal element of the 2x2 full CI Hamiltonian is $U_n(n_{p\uparrow}n_{p\downarrow}n_{p\uparrow}^vn_{p\downarrow}^v)^{1/2}$. The difference between the two diagonal elements is approximated in terms of the Fock matrix projected onto the transformed orbitals (eq 23 of ref ²⁶). Table SI1 shows that this approximation has a negligible effect on test molecules.

Projection States and Weights. I choose localized atom-centered projection states analogous to the states used in DFT+U. Just as in DFT+U, the results depend on the choice of projection state.²⁷ For each atom, I project the Kohn-Sham density matrix onto the valence atomic orbitals of the STO-3G minimal basis set. I choose the eigenvectors of this projected atomic density matrix as the projection states. Each projection state defines the electron-electron interaction operator for a different N-electron reference system (eq 1). Projection states on different atoms are typically nonorthogonal. Specialists may note that this is not “nonorthogonal CI”: each reference system simply includes a modified electron-electron interaction, and each reference system’s wavefunction is computed in the normal way. I choose the weights in eq 4 as the overlap of different projection states $w_n = \sum_m |\langle \phi_m | \phi_n \rangle|^{-2}$. With this, a projection state orthogonal to all others gets weight 1, and N identical and perfectly overlapping projection states each get weight 1/N. No matter what weights are used, there is no “double-counting” of correlation if the exact

functionals are available, because the correlation energy of the n th full CI wavefunction and the correction of the n th exact density functional sum to zero:

$$(5) 0 = E_{P,n}[\rho] - E_{KS}[\rho] \\ = \left(\min_{\Psi \rightarrow \rho} \langle \Psi | \hat{T} + \widehat{V}_{ee}^{P,n} | \Psi \rangle - \min_{\Phi \rightarrow \rho} \langle \Phi | \hat{T} | \Phi \rangle \right) + (E_{XC}^{P,n}[\rho] - E_{HXC}^{KS}[\rho])$$

Orbitals and Orbital Energies. All calculations use the self-consistent orbitals, orbital energies, and densities from the Kohn-Sham reference system. This choice ensures that all of the partially interacting reference systems have the same uncorrelated electron density. Figure SI1 shows how the choice of KS potential and KS orbital energies affects the partially interacting reference system correlation energies.

Projected Density Functionals. I test two approximate density functionals denoted PiFCI+HF and PiFCI+DFT. PiFCI+HF is analogous to CASSCF, and treats all of the XC functionals in eq 2-5 as nonlocal exact (Hartree-Fock) exchange. PiFCI+DFT is analogous to DFT-corrected CASSCF. PiFCI+DFT determines the Kohn-Sham orbitals & orbital energies with the Becke-Lee-Yang-Parr one-parameter global hybrid (25% exact exchange), and models the projected XC functionals as

$$(6) E_{XC}^{KS} + \sum_n w_n (E_{XC}^{P,n} - E_{XC}^{KS}) = E_{X,HF} + 0.2 (E_{X,LDA}^{P,full} - E_{X,HF}^{P,full}) + 0.8 E_{C,LYP} + 0.2 E_{C,LDA} + E(D3)$$

(Functionals' density dependence is omitted for conciseness.) This functional uses full exact exchange, LDA and Lee-Yang-Parr correlation,²⁸ D3 dispersion,²⁹ and 20% projected LDA exchange in the projection states. Functionals labeled "P,full" use the density matrix projected onto the full set of all projection states.³⁰ I use a local-hybrid-like *ansatz* to compute the projected LDA exchange energy, eq 15 of ref ³¹. Specialists may note that this functional includes 100% full exact exchange in density tails, atomic cores, and all regions outside of the STO-3G valence AO projection states.

Relation to Other Approximations. The literature on strong correlation is too large to cover comprehensively. I'll discuss six approximations that are particularly relevant to the present work. (1) CAS-in-DFT approximations use density functionals to add "dynamical" correlation to a multireference CAS wavefunction.³²⁻³³ The related multiconfigurational pair-density functional theory (MCPDFT) computes the full correlation energy from a pair-density functional.³⁴ The related λ -DFTB and multiconfigurational hybrid methods compute CAS or generalized valence bond wavefunctions for a single reference system employing a globally rescaled electron-electron interaction.³⁵⁻³⁶ These methods require an expensive non-black-box CAS calculation or a less expensive black-box valence-bond calculation on the entire active space. PiFCI+DFT, using the choices above, only requires two-determinant CI on the reference systems. PiFCI+DFT can recover a variant of CAS-in-DFT if one chooses a single partially-interacting reference system, in which the electron-electron interaction projected onto the entire active space.³⁷ (Table SI1 illustrates an example.) PiFCI+DFT can recover a variant of multiconfigurational hybrid methods if one chooses a single partially interacting reference system with $\widehat{V}_{ee}^P = \lambda \widehat{V}_{ee}$. (2) Selected CI methods compute approximate wavefunctions for large active spaces using deterministic selection (heat-bath CI,³⁸ DMRG-CAS,³⁹ DSRG⁸) or stochastic selection (quantum Monte Carlo⁴⁰) of "important" configurations. PiFCI instead selects "important" *projected interactions*, ensuring that each reference system can be treated with full CI. The approaches are complementary: one could imagine a "PiDMRG+DFT" in which the electron-electron interaction is projected onto a large active space, and e.g. DMRG-CAS is used to model the projected-interacting reference system wavefunction. (3) Local CI approximations employ localized orbitals to reduce the cost of

multiconfigurational calculations.⁴¹ PiFCI+DFT *localizes the interactions, not the orbitals*. The bottom panel of Figure 3 illustrates the difference: for this projected-interacting reference system, the projected electron-electron interaction is spatially localized, and the two transformed orbitals entering the full CI delocalize across the entire system. (4) DFT+U approximations use density functionals to correct the Hubbard model.²² The key difference is that, while multideterminant treatments of the Hubbard model are available,⁴² most modern DFT+U calculations simply use a single-configuration wavefunction and do not compute multireference correlation.⁴³ (5) Several modern DFT and DFT+U approximations satisfy the flat-plane condition and can treat strong correlation.^{14-15, 44-47} PiFCI+DFT grew out of my efforts to derive these methods from correlated wavefunction theory.²⁵ (6) Many *ab initio* and DFT approaches use symmetry breaking and restoration to “disentangle” entangled atoms.^{6, 48} PiFCI+DFT uses entangled, symmetrized wavefunctions throughout, with the hope that these will be useful for capturing entangled-atom physics.

Results

Figure 2a shows that PiFCI+DFT accurately treats N₂ dissociation. The bond energy near equilibrium is close to the NEVPT2 reference, and the energy at dissociation is almost perfectly zero. The density functional captures the “dynamical” correlation missing from PiFCI+HF, which underbinds near equilibrium. Figure 2b shows that PiFCI+DFT provides a reasonable dissociation curve for N₁₀₀. To my knowledge, this is the first application of a multiconfigurational wavefunction approximation to a 300-electron active space. PiFCI+DFT predicts that this square lattice N₁₀₀ has a relatively weak bond. The equilibrium lattice spacing 2.0 Å is about twice the N₂ bond length, and the equilibrium bond energy ~20 kcal/atom is about 15% that predicted for N₂. This is chemically reasonable: a nitrogen atom with four nearest-neighbor nitrogens would naïvely have an equilibrium bond energy around ¼ that of N₂. PiSCF+DFT correctly predicts that the interaction energy at dissociation is nearly zero: the energy of *entangled* spin-singlet dissociated N₁₀₀ almost perfectly matches the energy of 100 *unentangled* noninteracting nitrogen atoms. Figure S12 shows results for an evenly spaced chain of ten nitrogen atoms N₁₀. PiFCI+DFT predicts an equilibrium lattice spacing 1.5 Å and a bond energy ~25 kcal/atom midway between N₂ and N₁₀₀.

PiFCI calculations are fast. Computing the projected full CI correlation energy for 100 nitrogen atoms requires diagonalizing 100 4x4 projected atomic density matrices, then constructing and diagonalizing 400 2x2 CI matrices for the 400 projected-interacting reference systems. A single-shot PiFCI+HF total energy for N₁₀₀ takes less than 30 seconds wall time on a single 3000 MHz AMD EPYC-Milan processor.

PiFCI+DFT provides competitive accuracy for “normal” chemistry. Table 1 reports error statistics for PiFCI+DFT and two standard dispersion-corrected DFT methods, evaluated for subsets of the GMTKN55 benchmark dataset.⁴⁹ Table S12 reports detailed error statistics. PiFCI+DFT provides a weighted mean absolute deviation approaching dispersion-corrected PBE, while also effectively treating entanglement and strong correlation. In particular, PiFCI+DFT provides very low self-interaction error, with a SIE4x4 MAD well below dispersion-corrected B3LYP, consistent with its beyond-zero-sum performance (Figure S1).

PiFCI reference system wavefunctions encode information about entanglement and strong correlation. Table 2 shows that the reference systems’ projected occupancy and full CI correlation energy distinguish “normal”, entangled, and strongly correlated systems. “Normal” systems like H atom have occupancies near 1. The entangled system H₂⁺, the molecular analogue of the double-slit experiment, has fractional occupancies near ½. Dissociating symmetry-restricted singlet H₂ has

occupancies near $\frac{1}{2}$ and large correlation energies. Figure 1c shows this in action. Each nitrogen atom in the predicted equilibrium structure of N_{100} is colored by the full CI correlation energy from its associated reference systems. Values range from small (-0.12 au, blue) to large (-0.19 au, red). The “strong” correlation is strongest for the corner atoms and weakest for the central atoms. Figure 4 illustrates two other model systems, neutral and cationic octane with one dissociating C-C bond. Both bond dissociations produce entangled atoms. The neutral molecule, with two singlet-coupled electrons in the dissociating bond, also displays strong correlation.

Discussion

I believe that PiFCI+DFT is the first black-box multiconfigurational wavefunction method capable of routinely treating (at least) 100 entangled atoms and 300 active electrons. I believe that this promising result motivates further development. I'll conclude by discussing possible developments and prospects for the future.

Self-Consistency. The current implementation of PiFCI+DFT expands all reference system wavefunctions in a single set of molecular orbitals. This ensures that all reference systems have the same uncorrelated electron density. The first target for future work is self-consistent optimization of these orbitals. I hypothesize that the “strong” correlation captured by PiFCI+DFT will make it easier to converge single-determinant wavefunctions for strongly correlated states, mitigating variational collapse into un-entangled symmetry-broken states. I also note that the exact functionals would ensure that all reference systems the same *correlated* electron density. This could be a useful constraint on approximate projected functionals.

Solids. PiFCI+DFT has roots in DFT+U and should be readily extended to periodic systems. Specialists may note that, in DFT+U language, the electron-electron repulsion integral U_n in eq 1 is the nonempirical full (unscreened) U value. PiFCI+DFT does not require choosing or fitting a value of U.⁵⁰

Properties and Excited States. The key strength of PiFCI+DFT is that one does not compute the extremely expensive wavefunction for the interacting-electron entangled system. Properties of the real interacting-electron system must be computed as energy derivatives (as is typical in DFT), rather than as expectation values of the real system's wave function. Excited-state properties must be accessed by extending the exact (not linear response) time-dependent Kohn-Sham theory to treat partially interacting reference systems. I hypothesize that this extension will involve excited states of the partially interacting reference systems, just as time-dependent Kohn-Sham theory involves excited states of the noninteracting reference system. Work in this direction is underway.

Choice of Projected-Interacting Reference Systems. In this work, I choose to project the electron-electron interaction onto one localized state at a time (eq 1). Each reference system's correlated wavefunction captures (part of) the correlation energy of a singlet-coupled electron pair shared between the reference atom and one or more other atoms. This choice means that the reference systems' correlated wavefunctions do not capture all “important” correlation effects in all systems. While those effects *would be* captured by the exact projected density functionals, the limitations of approximate functionals might warrant different choices of reference system. I'll introduce four examples. (1) The wavefunctions of C_2 and stretched Cr_2 are not well described by a product of singlet-coupled, shared electron pairs.⁵¹⁻⁵² Test calculations (not shown) suggest that the current projected-interacting reference systems do not accurately treat C_2 and Cr_2 . (2) Ionizing an isolated atom typically changes one reference system's occupancy $n_{p\sigma}$ from near 1 to near 0,

such that the reference system correlation energy is very small. With these choices, PiFCI+HF atomic ionization potentials are very close to Hartree-Fock theory, thus the PiFCI+DFT ionization potentials in Table 1 are rather inaccurate. (3) Dispersion (van der Waals) interactions arise from coupled fluctuations on pairs of atoms, and cannot be captured one atom at a time. PiFCI+DFT includes D3 dispersion to capture this. (4) Projecting the electron-electron interaction operator onto a single state ensures that none of the reference systems include like-spin correlation.²⁶ Like-spin “strong” correlation can be important in some real systems.¹⁶ A natural and systematic way to capture all of these effects is to project the electron-electron interaction onto *pairs* of localized states. Work in this direction is underway.

Choice of Approximate Functionals. This work uses a DFT “exchange” functional, 20% projected LDA exchange, to capture some dynamical “correlation” effects. The DFT literature includes hundreds of approximate KS functionals, any of which can be converted into approximate projected-interacting functionals using the methods of ref³¹. It remains to be seen which of these approximations will work best. Approximate pair-density functionals developed for MCPDFT⁵³ might further reduce discrepancies between the wavefunction and DFT pieces (eq 5), though this approach goes outside the Hohenberg-Kohn theorems.

Overall, I believe that these results motivate vigorous exploration of projected-interacting reference systems to treat entangled atoms.

Materials and Methods

I have implemented PiFCI+DFT as an extension of the PySCF electronic structure package. The full implementation is freely available online at [github.org/bjaneko/CoreProjectedHybrids](https://github.com/bjaneko/CoreProjectedHybrids). Calculations on N₂ use the def2-TZVP basis set. Calculations on N₁₀ and N₁₀₀ use the def2-TZVP basis set, with Kohn-Sham orbitals obtained from Gaussian 16 DFT calculations using the LDA and the 3-21G basis set. The orbital energies entering the projected-interacting CI are obtained using 25% exact exchange. As discussed above, converging single-determinant self-consistent field calculations on entangled N₁₀ and N₁₀₀ was very difficult, as the calculations tended to collapse into artificially stabilized un-entangled states. LDA/3-21G was the only realistic option. Calculations on the GMTKN55 database use the aug-cc-pVQZ basis set with initial guesses from B3LYP/aug-cc-pVQZ calculations.

Acknowledgments

I acknowledge the TCU High-Performance Computing Center for computing resources.

References

1. Goyal, R. K.; Maharaj, S.; Kumar, P.; Chandrasekhar, M., Exploring quantum materials and applications: a review. *Journal of Materials Science: Materials in Engineering* **2025**, 20 (1), 4.
2. Bhandari, C.; Wysocki, A. L.; Economou, S. E.; Dev, P.; Park, K., Multiconfigurational study of the negatively charged nitrogen-vacancy center in diamond. *Physical Review B* **2021**, 103 (1), 014115.
3. Dong, X.; Del Re, L.; Toschi, A.; Gull, E., Mechanism of superconductivity in the Hubbard model at intermediate interaction strength. *Proceedings of the National Academy of Sciences* **2022**, 119 (33), e2205048119.

4. Perdew, J. P.; Ruzsinszky, A.; Constantin, L. A.; Sun, J.; Csonka, G. I., Some Fundamental Issues in Ground-State Density Functional Theory: I. Guide for the Perplexed. *J. Chem. Theory Comput.* **2009**, *5*, 902.
5. Angeli, C.; Cimiraglia, R.; Evangelisti, S.; Leininger, T.; Malrieu, J. P., Introduction of n-electron valence states for multireference perturbation theory. *The Journal of Chemical Physics* **2001**, *114* (23), 10252-10264.
6. Perdew, J. P.; Ruzsinszky, A.; Sun, J.; Nepal, N. K.; Kaplan, A. D., Interpretations of ground-state symmetry breaking and strong correlation in wavefunction and density functional theories. *Proceedings of the National Academy of Sciences* **2021**, *118* (4), e2017850118.
7. Zhang, J.; Pagano, G.; Hess, P. W.; Kyprianidis, A.; Becker, P.; Kaplan, H.; Gorshkov, A. V.; Gong, Z. X.; Monroe, C., Observation of a many-body dynamical phase transition with a 53-qubit quantum simulator. *Nature* **2017**, *551* (7682), 601-604.
8. Li, C.; Wang, X.; Zhai, H.; Fang, W.-H., Driven Similarity Renormalization Group with a Large Active Space: Applications to Oligoacenes, Zeaxanthin, and Chromium Dimer. *Journal of Chemical Theory and Computation* **2025**,
9. Örs Legeza, A. M., Ádám Ganyecz, Miklós Antal Werner, Kornél Kapás, Jeff Hammond, Sotiris S. Xantheas, Martin Ganahl, Frank Neese, Orbital optimization of large active spaces via AI-accelerators. *arXiv:2503.20700* **2025**,
10. Lieb, E. H., Density functionals for coulomb systems. *International Journal of Quantum Chemistry* **1983**, *24* (3), 243-277.
11. Levy, M., Electron densities in search of Hamiltonians. *Physical Review A* **1982**, *26* (3), 1200-1208.
12. Bowler, D. R.; Miyazaki, T., Calculations for millions of atoms with density functional theory: linear scaling shows its potential. *Journal of Physics: Condensed Matter* **2010**, *22* (7), 074207.
13. Sun, J.; Ruzsinszky, A.; Perdew, J. P., Strongly Constrained and Appropriately Normed Semilocal Density Functional. *Phys. Rev. Lett.* **2015**, *115*, 036402.
14. Bajaj, A.; Janet, J. P.; Kulik, H. J., Communication: Recovering the flat-plane condition in electronic structure theory at semi-local DFT cost. *The Journal of Chemical Physics* **2017**, *147* (19),
15. Burgess, A. C.; Linscott, E.; O'Regan, D. D., DFT+U-type functional derived to explicitly address the flat plane condition. *Physical Review B* **2023**, *107* (12), L121115.
16. Becke, A. D., Real-space post-Hartree-Fock correlation models. *Journal of Chemical Physics* **2005**, *122*, 64101.
17. Perdew, J. P.; Burke, K.; Ernzerhof, M., Generalized Gradient Approximation Made Simple. *Physical Review Letters* **1996**, *77* (18), 3865-3868.
18. Adamo, C.; Barone, V., Toward reliable density functional methods without adjustable parameters: The PBE0 model. *The Journal of Chemical Physics* **1999**, *110* (13), 6158-6170.
19. Ernzerhof, M.; Scuseria, G. E., Assessment of the Perdew–Burke–Ernzerhof exchange–correlation functional. *The Journal of Chemical Physics* **1999**, *110* (11), 5029-5036.
20. Janesko, B. G., Replacing hybrid density functional theory: motivation and recent advances. *Chemical Society Reviews* **2021**, *50* (15), 8470-8495.
21. Cohen, A. J.; Mori-Sanchez, P.; Yang, W. T., Challenges for density functional theory. *Chem. Rev.* **2012**, *112*, 289.
22. Kulik, H. J., Perspective: Treating electron over-delocalization with the DFT+U method. *J. Chem. Phys.* **2015**, *142*, 240902.

23. Stoll, H.; Savin, A., In *Density Functional Method in Physics* Dreizler, R. M.; Providencia, J. d., Eds. Plenum: Amsterdam, 1985; pp 177–207.
24. Toulouse, J.; Colonna, F.; Savin, A., Long-range--short-range separation of the electron-electron interaction in density-functional theory. *Physical Review A* **2004**, *70* (6), 062505.
25. Janesko, B. G., Adiabatic projection: Bridging ab initio, density functional, semiempirical, and embedding approximations. *The Journal of Chemical Physics* **2022**, *156* (1),
26. Janesko, B. G., Multiconfigurational Correlation at DFT + U Cost: On-Site Electron–Electron Interactions Yield a Block-Localized Configuration Interaction Hamiltonian. *The Journal of Physical Chemistry A* **2024**, *128* (25), 5077-5087.
27. Wang, Y.-C.; Chen, Z.-H.; Jiang, H., The local projection in the density functional theory plus U approach: A critical assessment. *The Journal of Chemical Physics* **2016**, *144* (14), 144106.
28. Lee, C.; Yang, W.; Parr, R. G., Development of the Colle-Salvetti correlation-energy formula into a functional of the electron density. *Physical Review B* **1988**, *37* (2), 785-789.
29. Grimme, S.; Antony, J.; Ehrlich, S.; Krieg, H., A consistent and accurate ab initio parametrization of density functional dispersion correction (DFT-D) for the 94 elements H-Pu. *J. Chem. Phys.* **2010**, *132*, 154104.
30. Janesko, B. G., Projected Hybrid Density Functionals: Method and Application to Core Electron Ionization. *Journal of Chemical Theory and Computation* **2023**, *19* (3), 837-847.
31. Janesko, B. G., Local hybrid alternatives to the orbital density approximation reduce the orbital dependence of self-interaction corrected DFT and the overbinding of DFT-corrected correlated wavefunctions. *The Journal of Chemical Physics* **2025**, *162* (11), 114113.
32. Gräfenstein, J.; Cremer, D., Development of a CAS-DFT method covering non-dynamical and dynamical electron correlation in a balanced way. *Molecular Physics* **2005**, *103* (2-3), 279-308.
33. Pijeu, S.; Hohenstein, E. G., Improved Complete Active Space Configuration Interaction Energies with a Simple Correction from Density Functional Theory. *Journal of Chemical Theory and Computation* **2017**, *13* (3), 1130-1146.
34. Gagliardi, L.; Truhlar, D. G.; Manni, G. L.; Carlson, R. K.; Hoyer, C. E.; Bao, J. W. L., Multiconfiguration Pair-Density Functional Theory: A new way to treat strongly correlated systems. *Acc. Chem. Res.* **2017**, *50*, 66.
35. Sharkas, K.; Savin, A.; Jensen, H. J. A.; Toulouse, J., A multiconfigurational hybrid density-functional theory. *The Journal of Chemical Physics* **2012**, *137* (4), 044104.
36. Ying, F.; Zhou, C.; Zheng, P.; Luan, J.; Su, P.; Wu, W., λ -Density Functional Valence Bond: A Valence Bond-Based Multiconfigurational Density Functional Theory With a Single Variable Hybrid Parameter. *Frontiers in Chemistry* **2019**, Volume 7 - 2019,
37. Rizo, L.; Janesko, B. G., Reimagining the Wave Function in Density Functional Theory: Exploring Strongly Correlated States in Pancake-Bonded Radical Dimers. *The Journal of Physical Chemistry A* **2023**, *127* (16), 3684-3691.
38. Holmes, A. A.; Tubman, N. M.; Umrigar, C. J., Heat-Bath Configuration Interaction: An Efficient Selected Configuration Interaction Algorithm Inspired by Heat-Bath Sampling. *Journal of Chemical Theory and Computation* **2016**, *12* (8), 3674-3680.
39. Yanai, T.; Kurashige, Y.; Neuscamman, E.; Chan, G. K.-L., Multireference quantum chemistry through a joint density matrix renormalization group and canonical transformation theory. *J. Chem. Phys.* **2010**, *132*,
40. Stella, L.; Attaccalite, C.; Sorella, S.; Rubio, A., Strong electronic correlation in the hydrogen chain: A variational Monte Carlo study. *Phys. Rev. B* **2011**, *84*, 245117.

41. Neese, F.; Hansen, A.; Wennmohs, F.; Grimme, S., Accurate Theoretical Chemistry with Coupled Pair Models. *Accounts of Chemical Research* **2009**, *42* (5), 641-648.
42. Ehlers, G.; White, S. R.; Noack, R. M., Hybrid-space density matrix renormalization group study of the doped two-dimensional Hubbard model. *Physical Review B* **2017**, *95* (12), 125125.
43. Gani, T. Z. H.; Kulik, H. J., Where Does the Density Localize? Convergent Behavior for Global Hybrids, Range Separation, and DFT+U. *Journal of Chemical Theory and Computation* **2016**, *12* (12), 5931-5945.
44. Wodyński, A.; Arbuznikov, A. V.; Kaupp, M., Strong-correlation density functionals made simple. *The Journal of Chemical Physics* **2023**, *158* (24),
45. Becke, A. D., A real-space model of nondynamical correlation. *Journal of Chemical Physics* **2003**, *119*, 2972.
46. Kong, J.; Proynov, E., Density functional model for nondynamic and strong correlation. *J. Chem. Theory Comput.* **2016**, *12*, 133.
47. Johnson, E. R.; Contreras-García, J., Communication: A density functional with accurate fractional-charge and fractional-spin behaviour for s-electrons. *The Journal of Chemical Physics* **2011**, *135* (8), 081103.
48. Shen, J.; Xu, E.; Kou, Z.; Li, S., New coupled cluster approaches based on the unrestricted Hartree–Fock reference for treating molecules with multireference character. *Physical Chemistry Chemical Physics* **2011**, *13* (19), 8795-8804.
49. Goerigk, L.; Hansen, A.; Bauer, C.; Ehrlich, S.; Najibi, A.; Grimme, S., A look at the density functional theory zoo with the advanced GMTKN55 database for general main group thermochemistry, kinetics and noncovalent interactions. *Physical Chemistry Chemical Physics* **2017**, *19* (48), 32184-32215.
50. Allam, N. K.; Tolba, S. A.; Gameel, K. M.; Ali, B. A.; Almossalami, H. A., The DFT+U: Approaches, Accuracy, and Applications. In *Density Functional Calculations - Recent Progresses of Theory and Application*, Yang, G., Ed. IntechOpen: Rijeka, 2018.
51. Xu, L. T.; Dunning, T. H., Jr., Insights into the Perplexing Nature of the Bonding in C₂ from Generalized Valence Bond Calculations. *Journal of Chemical Theory and Computation* **2014**, *10* (1), 195-201.
52. Larsson, H. R.; Zhai, H.; Umrigar, C. J.; Chan, G. K.-L., The Chromium Dimer: Closing a Chapter of Quantum Chemistry. *Journal of the American Chemical Society* **2022**, *144* (35), 15932-15937.
53. Li Manni, G.; Carlson, R. K.; Luo, S.; Ma, D.; Olsen, J.; Truhlar, D. G.; Gagliardi, L., Multiconfiguration Pair-Density Functional Theory. *Journal of Chemical Theory and Computation* **2014**, *10* (9), 3669-3680.

Figures and Tables

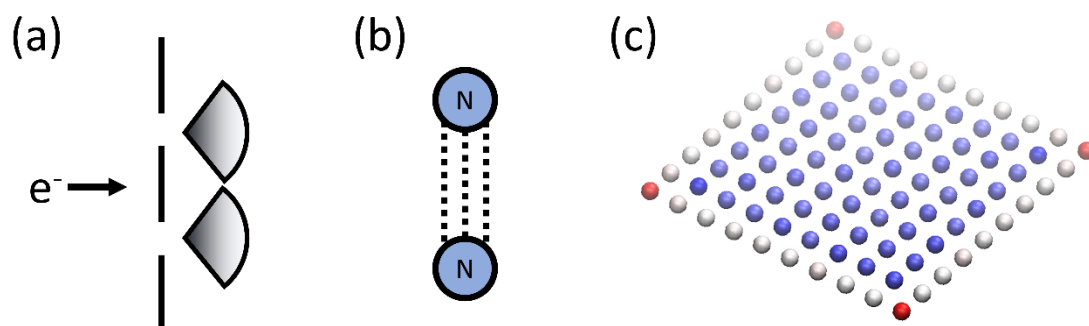


Figure 1. Entangled quantum systems. (a) Double-slit experiment. (b) Dissociating nitrogen molecule N_2 . (c) Dissociating singlet N_{100} as treated here. Atoms in Figure 1c are colored by the magnitude of "strong" correlation, from large (red) to small (blue).

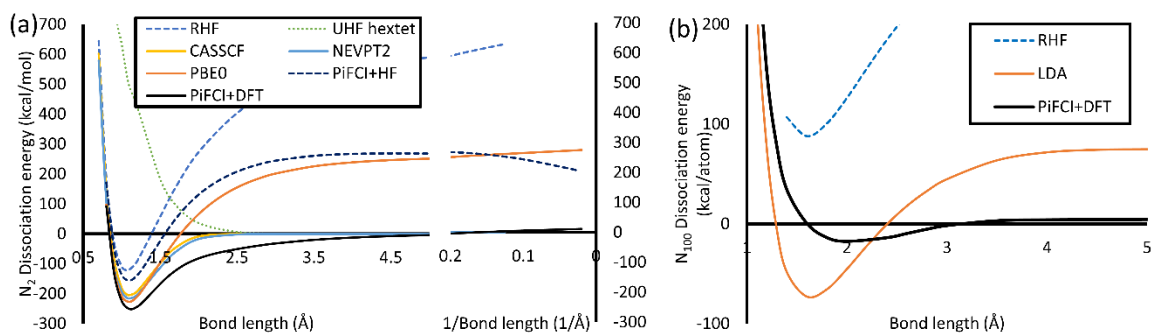


Figure 2. Computed potential energy surfaces. (a) Dissociating N_2 . (b) Dissociating N_{100} .

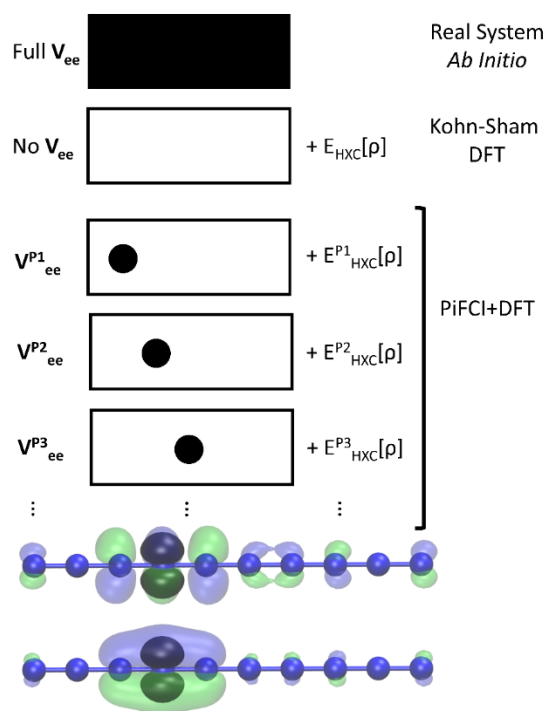


Figure 3. Cartoon of PiFCI+DFT. *Ab initio* wavefunction theory treats a real system of fully interacting electrons (top). Kohn-Sham DFT treats a reference system of noninteracting electrons corrected by a density functional. PiFCI+DFT treats multiple reference systems of *partially*-interacting electrons, each corrected by a projected density functional. Given the exact functionals, any combination of the partially-interacting systems' ground-state densities and energies recovers the exact results. The lower panels illustrate one of the 40 reference systems from a PiFCI+DFT calculation on N_{10} . The projection state for electron-electron interactions is in black, and the transformed virtual (top) and occupied (bottom) orbitals used in the two-determinant full CI are in blue and orange.

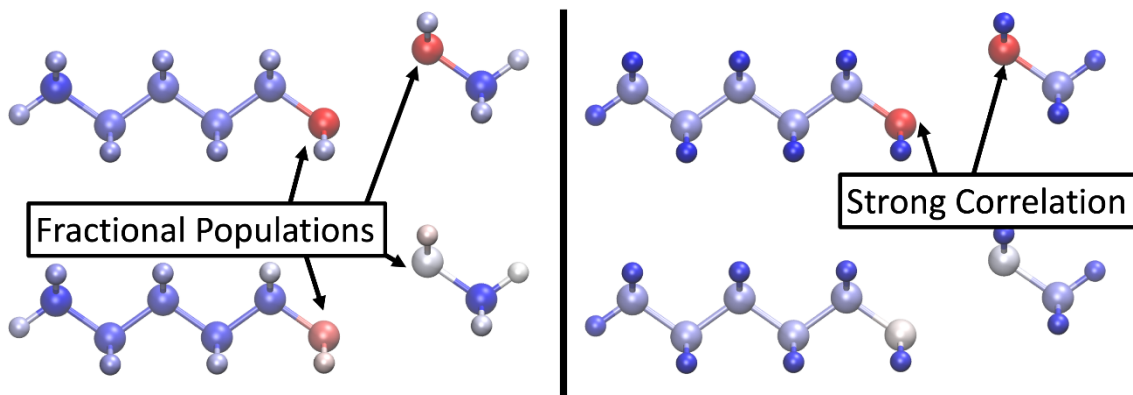


Figure 4. Dissociating neutral (top) and cationic (bottom) octane molecule. Each atom is colored by the associated projected-interacting reference systems average occupancy (left) or summed full CI correlation energies (right). Red denotes occupancy near $\frac{1}{2}$ (left) or large correlation energy (right).

Dataset	PBE-D3(BJ)	B3LYP-D3(BJ)	PiFCI+DFT
Cumulative	8.36	5.05	9.66
W4-11 atomization energy	15.7	3.4	13.2
G21IP ionization potential	3.85	3.55	5.50
SIE 4x4 self-interaction error	23.72	18.06	4.83
RSE43 radical stabilization	2.94	1.72	1.97
BH76 barrier height	9.62	5.70	4.47

Table 1. Mean absolute errors MAE for representative databases of the GMTKN55 benchmark dataset, and cumulative WTMAD-2 for 45 subdatabases (see SI). B3LYP-D3(BJ) and PBE-D3(BJ) results are from ref ⁴⁹.

Classification	System	Population	Correlation energy
"Normal"	Isolated H atom	0.96	0
	Equilibrium H_2^+	0.72	0
	Equilibrium H_2	0.82	5
Entangled	Stretched H_2^+	0.49	0
Entangled and strongly correlated	Stretched H_2	0.46	117

Table 2. Average majority-spin population (unitless) and full CI correlation energy (milli-Hartree) for "normal", entangled, and strongly correlated model systems.

Supporting Information

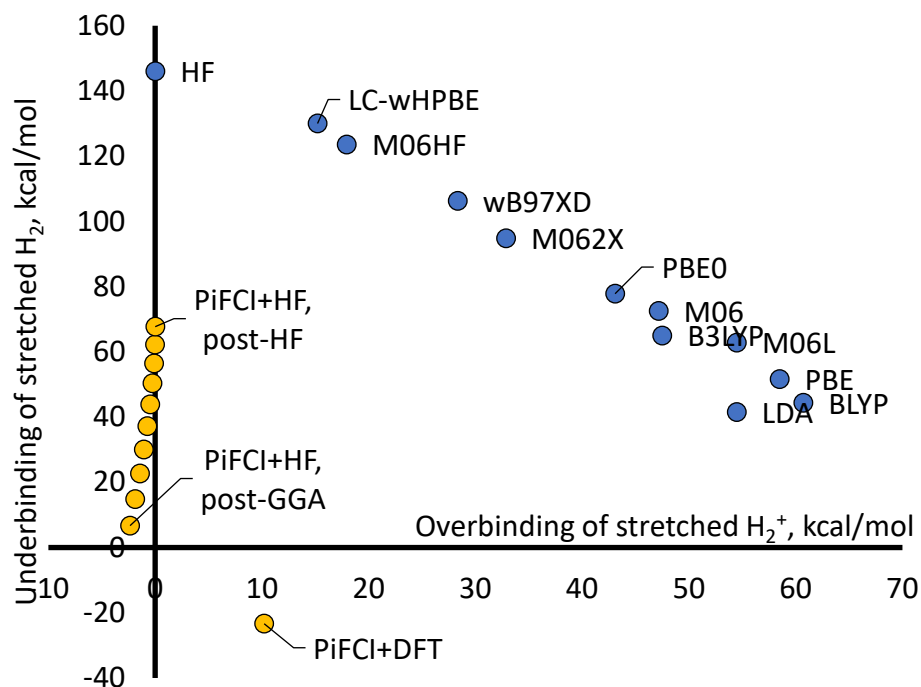


Fig. S1. Zero-sum tradeoffs in the bond energy of stretched H_2^+ and stretched singlet spin-symmetry-restricted H_2 . Calculations using the def2-TZVP AO basis set. Standard DFT approximations either over-delocalize H_2^+ or underbind H_2 . PiFCI+DFT provides very accurate results, with modest overbinding of stretched H_2 . The different points labeled PiFCI+HF points show the effect of changing the Kohn-Sham orbitals and orbital energies entering the reference system CI Hamiltonian. Kohn-Sham orbitals computed using a small (large) fraction of exact exchange give a small (large) HOMO-LUMO gap and correspondingly large (small) reference system correlation energies.

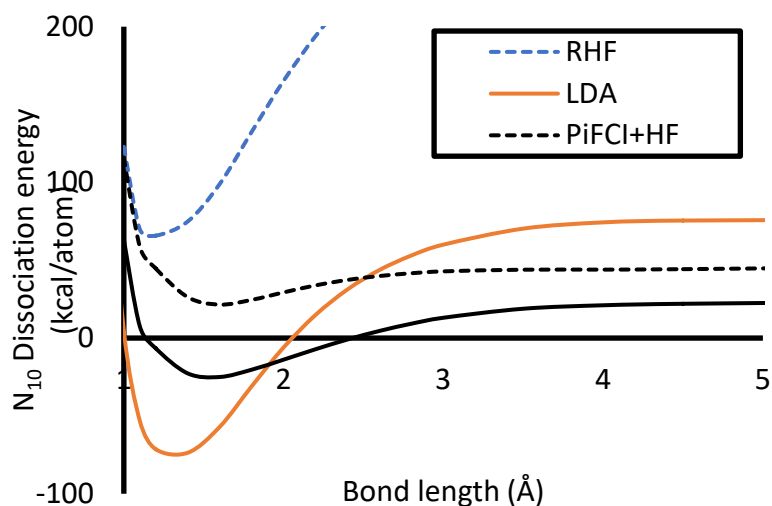


Fig. S2. Dissociation curve for linear spin-singlet N_{10} chain.

				PiFCI+HF		
Basis set for MOs	System	Hartree-Fock	Full CI	Approximate diagonal element	Exact diagonal element	Full valence projection
STO-3G	H atom	-0.466582	-0.466582	-0.466582	-0.466582	-0.466582
	H ₂ , R _{HH} =0.74 Å	-1.116759	-1.137284	-1.121392		-1.137284
	H ₂ , R _{HH} =1.2 Å	-1.005107	-1.056741	-1.031427	-1.030208	-1.056741
	H ₂ , R _{HH} =10 Å	-0.572320	-0.933164	-0.867987	-0.867987	-0.933164
	H ₂ , R _{HH} =60 Å	-0.550271	-0.933164	-0.920333	-0.920344	-0.933164
aug-cc-pVTZ	H atom	-0.499821	-0.499821	-0.499821	-0.499821	-0.499821
	H ₂ , R _{HH} =0.74 Å	-1.133034	-1.172630	-1.137767	-1.137285	-1.153496
	H ₂ , R _{HH} =1.2 Å	-1.063040	-1.112790	-1.089750	-1.088698	-1.110441
	H ₂ , R _{HH} =10 Å	-0.741525	-0.999643	-0.894788	-0.893939	-0.990018
	H ₂ , R _{HH} =60 Å	-0.719456	-0.999642	-0.897555	-0.896712	-0.990457

Table S1. Total energies (Hartree atomic units) for H atom and H₂. PiFCI+HF is exact within a given basis set for H atom. PiFCI+HF using the exactly computed reference system CI Hamiltonian, versus the approximate diagonal element used in the rest of this paper, give nearly identical results. “Full valence projection” denotes PiFCI+HF using a single reference system, in which the electron-electron interaction operator is projected onto the entire set of STO-3G valence AOs. If the MOs are also computed in the STO-3G minimal basis set, PiFCI+HF recovers the exact energy at large R_{HH} and converges as R_{HH}⁻¹ towards that limit. Full valence projection recovers full CI at all bond lengths. If the MOs are computed in the larger aug-cc-pVTZ basis set, PiFCI+HF is missing “dynamical” correlation relative to full CI.

Dataset	Number entries	MD	MAD	RMSD	Max
W4-11	140	-1.85	13.174	17.41	44.29
G21EA	24	-7.62	8.788	10.76	20.98
G21IP	36	0.32	5.5	7.68	22.29
DIPCS10	10	-8.18	11.236	12.6	24.96
PA26	26	3.56	3.908	4.78	12.49
SIE4x4	16	-2.87	4.834	5.81	10.47
ALKBDE10	10	-10.62	11.391	13.41	21.74
YBDE18	18	-3.4	3.943	6.26	19.78
AL2X6	6	2.21	2.209	2.42	4.16
HEAVYSB11	11	-4.13	5.658	6.2	8.92
NBPRC	12	-1.93	4.501	5.3	8.56
ALK8	8	-6.42	6.421	9.68	19.52
RC21	21	-11.36	13.728	17.95	45.59
G2RC	25	4.65	12.723	15.93	36.91
BH76RC	30	0.75	5.115	8.89	35.97
FH51	51	5.94	8.947	13.19	47.89
TAUT15	15	0.45	2.801	3.51	6.82
DC13	13	3.01	32.486	43.05	85.67
MB16-43	43	-42.34	47.68	56.6	133
DARC	14	32.89	32.889	33.29	43.19
RSE43	43	-0.93	1.969	2.93	12.79
BSR36	36	-3.52	3.522	4.6	13.42
CDIE20	20	-3.03	3.382	4.09	7.24
ISO34	34	1.01	5.683	8.88	21.84
PArel	20	-0.51	2.074	2.62	6.05
BH76	76	-1.35	4.469	6.47	29.82
BHPERI	26	13.36	14.685	15.33	24.6
BHDIV10	10	4.79	6.723	9.25	20.22

INV24	24	0.64	4.42	6.57	22.31
BHROT27	27	-0.5	0.633	1.25	4.46
PX13	13	5.22	5.217	5.38	7.33
WCPT18	18	7.59	7.594	7.88	11.47
RG18	18	0.26	0.256	0.35	1.11
ADIM6	6	0.96	0.964	1.01	1.42
S22	22	0.01	0.576	0.66	1.47
S66	66	0.39	0.539	0.6	1.23
HEAVY28	27	-0.25	0.402	0.52	1.39
WATER27	27	13.38	13.383	17.4	39.9
CARBHB12	12	0.18	0.462	0.5	0.88
PNICO23	23	0.58	0.651	0.8	2.33
HAL59	59	-0.16	0.643	1.02	3.86
AHB21	21	-1.41	2.007	2.3	4.35
CHB6	6	-1.66	3.132	3.64	6.51
IL16	15	-0.23	0.7	0.92	2.27
ACONF	15	-0.17	0.167	0.2	0.4

Table S2. PiFCI+DFT error statistics (kcal/mol) for 45 subdatabases of the GMTKN55 database. MD denotes mean deviation, MAD denotes mean absolute deviation, RMSD denotes root-mean-square deviation, Max denotes maximum